Article

Sulfur Hexafluoride (SF$_6$) Plasma Treatment of Medical Grade Poly(methyl methacrylate)

Stefano Zanini [1], Antonio Papagni [2], Luca Vaghi [2,*], Baljit Kaur Thatti [3,*], Stephen Barton [3], Neil Williams [3], Navid Shokri [3] and Claudia Riccardi [1]

[1] Dipartimento di Fisica "G. Occhialini", Università degli Studi di Milano-Bicocca, Piazza della Scienza 3, I-20126 Milano, Italy; stefano.zanini@unimib.it (S.Z.); claudia.riccardi@unimib.it (C.R.)

[2] Dipartimento di Scienza dei Materiali, Università degli Studi di Milano-Bicocca, Via Roberto Cozzi 55, I-20125 Milano, Italy; antonio.papagni@unimib.it

[3] Department of Chemical and Pharmaceutical Sciences, Kingston University, Penrhyn Road, Kingston Upon Thames, Surrey KT1 2EE, UK; S.barton@kingston.ac.uk (S.B.); N.a.williams@kingston.ac.uk (N.W.); k0915601@kingston.ac.uk (N.S.)

* Correspondence: luca.vaghi@unimib.it (L.V.); B.Thatti@kingston.ac.uk (B.K.T.)

Abstract: Medical-grade poly(methyl methacrylate) (PMMA) is widely employed in the fabrication of intraocular lenses (IOLs), but suffers from opacification, a postoperative complication that leads to the failure of the implanted intraocular lenses. The opacification occurs when inorganic-based deposits accumulate on the surface of the IOL and are prevalent in hydrophilic materials. Here, the surface of medical-grade PMMA has been fluorinated by sulphur hexafluoride (SF$_6$) plasma treatment to increase surface hydrophobicity thus improving the material lifetime in optical applications. Hydrophobic properties of the treated PMMA were investigated by means of contact angle measurements, while chemical modification was assessed by X-ray Photoelectron Spectroscopy (XPS) and Attenuated Total Reflectance Fourier Transform Infrared (ATR/FTIR) spectroscopy. Surface morphological changes due to possible etching effects were investigated by Atomic Force Microscopy (AFM). The transparency of the treated PMMA was assessed by UV/VIS spectroscopy. Finally, the influence of the plasma treatment on the inorganic salts deposition was investigated by immersion in Simulated Aqueous Humour (SAH), followed by XPS analysis. The modified samples showed less deposition on the surface than the unmodified sample, moreover, a decrease of the transmittance in the UV-violet range (300–430 nm) was detected, open the possibility of interesting applications of this treatment for the creation of a UV filter in ophthalmic optical devices.

Keywords: poly(methyl methacrylate) (PMMA); sulfur hexafluoride; plasma treatment; opacification; simulated aqueous humour (SAH); intraocular lenses

1. Introduction

Crystalline clouding (cataract) is usually corrected by replacing the opaque crystalline lens with intraocular lenses (IOLs). Poly(methyl methacrylate) PMMA was used for the first IOL implantation by Harold Ridley in 1949 and remains the reference material with which new materials proposed for intraocular lenses are compared [1]. Even though in some countries, to reduce trauma to the eye during surgery, PMMA implants are being replaced by foldable hydrophilic and silicone IOLs, PMMA IOLs are still widely used, especially in the developing world.

Opacification of IOLs occurs when calcium, sodium and potassium-containing deposits build upon their surface. This complication was reported as early as 1999 and results in a failure of the IOL implant following cataract surgery [2–6]. Opacification is a problem of growing concern because the

failed implant must be removed incurring considerable costs and repeat trauma to the eyes of the patient.

This phenomenon is more consistent with hydrophilic IOLs (made up of a copolymer of hydroxyethyl methacrylate and methyl methacrylate), possibly due to the capability of hydroxyl ethyl carboxylic esters at the surface to complex calcium ions creating nucleation centres that trigger the growth of the crystallites [7]. However, to date, there is no consensus within the scientific community on a reasonable mechanism for its formation.

It has been observed that water may diffuse/absorb into the polymer network, due to the existence of significant free volume (void spaces). Previous studies have shown that water diffusion can trigger the opacification process, providing a more favourable environment for the formation and the adhesion of the inorganic deposits. Therefore, hindering water diffusion may in turn help to delay opacification, or even prevent it. Water diffusion is favoured by hydrogen bonding with the oxygen of MMA carboxylic ester functional groups [8] thus the reduction of the surface polarity (for example by means of fluorination) is thought to limit this phenomenon and subsequently to slow down or to inhibit the opacification process.

This hypothesis has been tested and its validity proved in previous works, where the direct surface plasma fluorination of PMMA IOLs employing F_2 or exploiting surface segregation of perfluoroalkyl chains effectively hinder the surface formation of inorganic-based deposits [9,10]. As discussed above, this was attributed to the barrier effect of the hydrophobic, fluorinated PMMA surface, which caused a slower rate of diffusion of water into the polymer network, compared with the untreated PMMA. However, surface fluorination with fluorine gas is too aggressive and gravimetric analyses underline a significant structural degradation in the PMMA surface.

Among the several techniques for the surface modification of polymeric materials, plasma treatment is one of the most largely employed, since it offers several major advantages over other methods. Plasma is a suitable technique since it modifies only the surface of the materials, without affecting their physical and chemical bulk properties. Moreover, the fine-tuning of the treatment parameters (gas pressure, exposure time, power) allows "soft" modifications, that affect in a negligible way the surface roughness. To limit the surface roughness results in a reduction of light scattering and this is particularly important in optical devices such as IOLs, where preserving the transparency in modified materials is essential and need to be guaranteed. In the biomedical field, low-pressure plasma treatment and plasma polymerization are often used for the introduction of different reactive functionalities (i.e., COOH, OH, oxazoline and NH_2 groups) onto otherwise inert surfaces [11–14]. The plasma-modified surfaces can be directly exploited to control bio-interfacial interactions or used as anchorage sites for the covalent immobilization of specific biomolecules. In other cases, plasma treatments are employed to modify the surface energy and the water wettability of polymeric materials, by the introduction of hydrophilic (OH, COOH) or hydrophobic (F, CF_3) groups [13,15,16].

In this work, surface fluorination of medical-grade PMMA has been performed by sulfur hexafluoride (SF_6) plasma treatment. It has been shown that surface fluorination, with fluorine inserted in the polymer chain, can be achieved by exposing polymeric surfaces to SF_6 low-pressure discharges under appropriate conditions [17]. In the past, we have found evidence of surface fluorination of different natural and artificial polymeric surfaces, such as poly(ethylene terephthalate) (PET), cotton and silk [15,18]. As expected, fluorinated surfaces exhibited lower wettability than their untreated counterparts.

Here, the hydrophobic properties of the treated PMMA were investigated by contact angle measurements. Chemical modification arising from the plasma treatment was assessed by X-ray Photoelectron Spectroscopy (XPS) and Attenuated Total Reflectance Fourier Transform Infrared (ATR/FTIR) spectroscopy. Surface morphological changes due to possible etching effects were investigated by Atomic Force Microscopy (AFM), the transparency of the treated PMMA was assessed by UV/VIS spectroscopy. Finally, the influence of the plasma treatment on the opacification was investigated by immersion in Simulated Aqueous Humour (SAH), followed by XPS analysis.

2. Materials and Methods

2.1. Materials

High molar mass medical-grade PMMA discs (2.5 mm thickness and 10 mm diameter, Evonik, Milton Keynes, UK) were used in this study. SF_6 was obtained from Sapio (purity > 99.95%). The materials used for the simulated aqueous humour [19] were as follows, Phosphate Buffered Saline (PBS) tablets (Fisher Scientific), NaCl, $HCl_{(aq)}$, $NaHCO_3$, KCl, $MgCl_2 \cdot 6H_2O$, Na_3PO_4, $CaCl_2 \cdot 2H_2O$, Na_2SO_4, Urea, glucose, alanine, lysine, serine and valine (Sigma-Aldrich Co, Gillingham, UK), sodium lactate and sodium hyaluronate (Alfa Aesar, Heysham, UK).

2.2. Plasma Reactor and Plasma Modification of PMMA IOLs

Plasma treatment was performed in a parallel-plates plasma reactor, which has been previously described [11,20]. Before every plasma treatment, the reactor was evacuated to 10^{-3} Pa by means of a rotary pump combined with a turbo-molecular pump. Then, SF_6 was introduced in the chamber by means of a needle valve and was uniformly distributed in the reactor by the upper showerhead electrode (with pinholes diameter of 2 mm). This electrode was connected to a 13.56 MHz RF power supplier (Advanced Energy RFX-600, Mouser Electronics, Assago, Italy) which provided an RF voltage towards the grounded chamber. The lower grounded electrode was used as a sample holder. All plasma treatments were performed in pulsed mode, with a frequency of 500 Hz and a duty cycle (DC = $t_{ON}/(t_{ON} + t_{OFF})$) of 50% ($t_{ON}$: 1 ms, t_{OFF}: 1 ms). The RF peak power and the SF_6 pressure were varied to maximize the hydrophobic characteristics of the treated lenses. For this purpose, two sets of experiments were performed. In the first set, plasma treatments were carried out at a fixed peak power of 70 W, while the SF_6 pressure was varied between 5 and 50 Pa. In the second set, the SF_6 pressure was fixed at 30 Pa and the peak power input was varied between 50 and 110 W. In all these experiments, the total duration of the treatment ($t_{ON} + t_{OFF}$) was fixed to 5 min.

2.3. Characterization Techniques

The effect of the plasma treatment on the IOLs wettability was assessed by means of dynamic contact angle measurements with a Dataphysics OCA 20 (Dataphysics) instrument. The measurements were performed at room temperature. The data reported are the average of 4 measures each sample.

Chemical modification of the PMMA IOLs was assessed by means of a Fourier transform infrared (FT-IR) spectrometer (Nicolet iS10, Thermo Scientific, Rodano, Italy) equipped with an ATR sampling accessory (Smart iTR, Thermo Scientific, Rodano, Italy). For each spectrum 32 scans were recorded, with a spectral resolution of 2 cm^{-1}. All spectra were acquired within a few hours from the plasma treatment. The interpretation was performed by subtracting the spectrum of the untreated PMMA from the spectra of the plasma-treated samples.

XPS analysis was performed using a PerkinElmer Φ 5600-ci spectrometer and Al Kα radiation (1486.6 eV). The sample analysis area was 800 μm in diameter. Survey scans were obtained in the 0–1350 eV range (187.8 eV pass energy, 0.8 eV step-1, 0.05 sec step-1). Detailed scans were recorded for the C1s, O1s and F1s (23.5 eV pass energy, 0.1 eV step-1, 0.1 sec step-1). The standard deviation for the BEs values is ± 0.2 eV. The experimental uncertainty on the reported atomic composition values does not exceed ± 5%. The XPS spectrometer was calibrated by assuming the binding energy (BE) of the Au 4f7/2 line at 83.9 eV with respect to the Fermi level. The BE shifts were corrected by assigning to the C1s peak associated with adventitious hydrocarbons a value of 284.8 eV [21]. Samples were mounted on steel holders and introduced directly in the fast-entry lock system of the XPS analytical chamber. The data analysis involved Shirley-type background subtraction, non-linear least-squares curve fitting adopting Gaussian-Lorentzian peak shapes, and peak area determination by integration [22]. The atomic compositions were evaluated from peak areas using sensitivity factors supplied by PerkinElmer (Beaconsfield, UK), considering the geometric configuration of the apparatus [23].

Topographical modifications owing to the plasma treatment were investigated by means of Atomic Force Microscopy (AFM). AFM measurements were carried out using a Solver P47-PRO (NT-MDT, Moscow, Russia), in semi-contact mode. HA_NC (High Accuracy Non-Contact) silicon tips (NT-MDT) with typical spring constant $5.8 \pm 20\%$ N/m and resonance frequency $200 \pm 10\%$ kHz were used. Square images (30 μm × 30 μm and 10 μm × 10 μm) were collected at a typical scan frequency of 1.5 Hz and with 256 points per line.

Optical transparency of the plasma-treated lenses was assessed by means of UV/VIS analyses (UV-2101 PC spectrophotometer, Shimadzu Italia, Milano, Italy). Spectra were acquired in the 300-800 nm range.

2.4. Immersion in SAH

The SAH was prepared following in detail the procedure described by Chirila et al. [19].

The samples used for the immersion study were treated once a day with SF_6 plasma, for 5 days. In these five days, samples A1 and A2 were stored in air at room temperature, while samples B1 and B2 were stored in an oven at 50°C (with a beaker of water, in order to increase the humidity).

Next, the PMMA discs (control, A1, A2, B1 and B2) were placed separately into sterile sample tubes, 10 mL of SAH was then added into each tube. The tubes were then placed in the oven at 37 °C for 8 weeks. At the end of that period the PMMA discs were removed from the sample tubes, gently patted dry for 1 s on each side and placed into new sterile sample tubes ready for XPS analysis.

XPS analysis post immersion. XPS analyses were performed on a ThermoFisher Scientific Instruments (East Grinstead, UK) K-Alpha+ spectrometer. XPS spectra were acquired using a monochromatic Al Kα X-ray source (h = 1486.6 eV). An X-ray spot of ~400 μm radius was employed. Survey spectra were acquired employing a Pass Energy of 200 eV. High resolution, core-level spectra for all elements were acquired with a Pass Energy of 50 eV. Quantitative surface chemical analyses were calculated from the high resolution, core level spectra following the removal of a non-linear (Shirley) background. The manufacturer's Avantage software was used which incorporates the appropriate sensitivity factors and corrects for the electron energy analyser transmission function.

3. Results and Discussion

3.1. SF$_6$ Plasma Treatment and Characterization

3.1.1. Influence of SF$_6$ Pressure

Figure 1 shows the advancing and receding contact angles measured onto the plasma-treated IOLs as a function of the SF_6 pressure (peak power = 70 W, DC = 50%). In the same graph, two horizontal dashed lines represent the values of the untreated PMMA. Three distinct zones can be observed. Hydrophobic characteristics of the treated lenses increased with the SF_6 pressure in the range 5-20 Pa, while they did not significantly change in the range 20–35 Pa. Moreover, a strong decrease of both advancing and receding contact angles was observed by further increasing the SF_6 pressure up to 50 Pa. Notably, treatments performed at 5 and 50 Pa increased the wettability of the PMMA lenses with respect to the untreated ones.
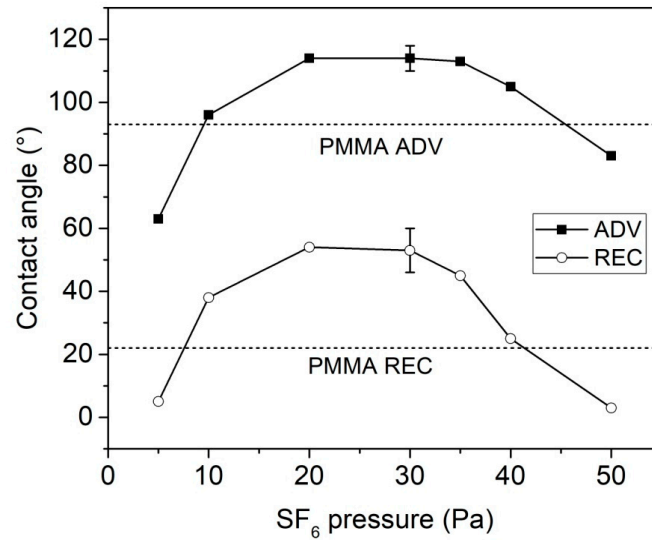
Figure 1. Advancing and receding contact angles of plasma-treated intraocular lenses (IOLs) as a function of the SF$_6$ pressure (peak power = 70 W, DC = 50%). The two horizontal dashed lines represent the values of the untreated poly(methyl methacrylate) (PMMA).

The increase in wettability observed at the lower SF$_6$ pressure (5 Pa) is in agreement with our previous work on other polymeric surfaces (cellulose, poly(ethylene terephthalate) [17]. Instead, plasma treatment performed at higher pressures (10–40 Pa) increased the surface hydro-repellence, due to extended surface fluorination.

Returning to the plasma treatment of PMMA IOLs, the FTIR/ATR analyses confirmed the surface activation of the samples prepared at low pressure and the fluorination of those prepared at 20-35 Pa. The FTIR/ATR spectra of two lenses modified at 5 Pa and 30 Pa (peak power = 70 W, DC = 50%) are displayed in Figure 2.
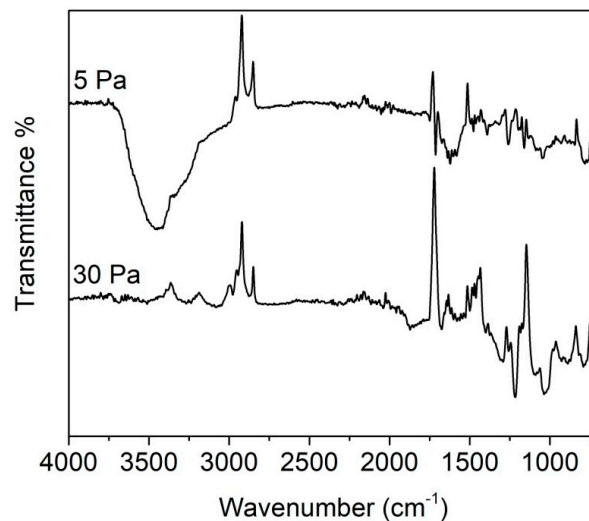

Figure 2. Attenuated Total Reflectance Fourier Transform Infrared (ATR/FTIR)spectra of PMMA IOLs treated at different SF$_6$ pressures (peak power = 70 W, DC = 50%). Displayed spectra were obtained by subtracting the spectrum of the untreated PMMA to the spectra of the treated samples.

As explained in the experimental section, to evidence the effects of the plasma treatment the spectrum of untreated PMMA was subtracted from the spectrum of the treated sample. In fact, by

simply comparing the spectra of the plasma-treated and the untreated PMMA, it was very difficult to detect any differences. This result indicates that plasma activation and fluorination interest only the outermost layers of the polymeric samples, as can be expected considering the mild character of this modification technique.

In the IR spectrum of the sample treated at 5 Pa, a strong band centred at 3300 cm^{-1} appeared. This peak can be attributed to O-H group stretching vibrations. This suggests that at low SF$_6$ pressure (i.e., at low density of fluorine radicals in the plasma phase) the main process is the formation of radicals due to plasma species bombardment. Which when exposed to air react with atmospheric oxygen giving peroxy radicals, and subsequently hydroperoxide groups, which in turn can decompose into oxygenating species such as hydroxyl groups.

The spectrum of the sample treated at 30 Pa displays several bands in the range 1000-1300 cm^{-1}, which can be attributed to the presence of fluorinated species (CF, CF$_2$ and CF$_3$ groups) [24]. These species derive from the surface fluorination of the PMMA, with substitution of the hydrogen atoms in CH$_x$ groups with fluorine. Both samples display a decrease in intensity of the bands at 1720 cm^{-1} (C=O groups of methacrylate) and 2800–3000 cm^{-1} (CH$_x$ groups), as indicated by the negative peaks in the subtraction spectra of Figure 2. This indicates loss of CH$_x$ and C=O groups, due to surface fluorination (or to the grafting of oxygenated species like hydroxyls) and to the partial loss of the lateral chains of the PMMA. Moreover, in the sample treated at 30 Pa has observed a strong decrease of the band near 1200 cm^{-1} (C–O stretching), this means that at this pressure also the methoxy groups are lost.

3.1.2. Influence of RF Peak Power

Figure 3 shows the influence of the RF peak power on the hydrophobic properties of the plasma-treated PMMA samples (SF$_6$ pressure = 30 Pa, DC = 50%). The results indicate that within the range we have investigated the effect of RF peak power is negligible, although a slight decrease of both advancing and receding contact angles was observed by increasing the RF power.
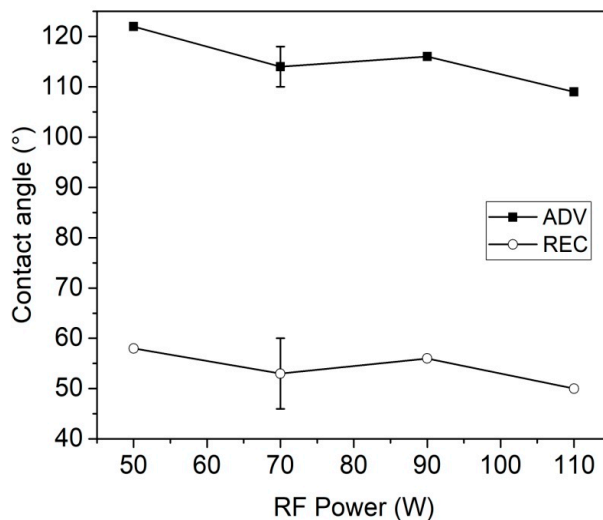

Figure 3. Advancing and receding contact angles of plasma-treated IOLs as a function of the RF peak power (SF$_6$ pressure = 30 Pa, DC = 50%).

It is clear in Figures 1 and 3 that plasma treatments at pressures of 20-30 Pa and with peak powers between 50 and 90 W can considerably increase the hydrophobic properties of the PMMA lenses., The low intensity of the CF$_x$ bands in the FTIR/ATR spectra (owing to the low penetration depth of the plasma modification) did not allow any analysis of the extent of fluorination.

3.1.3. XPS Analysis

The amount of surface fluorine in the treated samples was investigated by means of XPS analysis. Table 1 shows the atomic percentage of elements measured on samples prepared in different ways, together with results of the deconvolution of the C1s and O1s peaks. The atomic percentages of elements measured on the untreated PMMA are close to the theoretical ones, although we observed a slightly lower oxygen content (about 90% of the theoretical value).

Table 1. X-ray Photoelectron Spectroscopy (XPS) data for untreated and plasma-treated PMMA samples.

SAMPLE	% C							% O			% F
	C–C	C–O (C–CF$_3$)	O–C=O (C–F)	CF$_2$	CF$_3$	O–CF$_3$	C–TOT	C–O	C=O	O TOT	
Untreated PMMA Theoretical	42.9	14.3	14.3	-	-	-	71.4	14.3	14.3	28.6	-
Untreated PMMA Measured	49.3	12.6	12.5	-	-	-	74.5	13.8	11.7	25.5	-
Fluorinated PMMA Theoretical	-	6.7	6.7	6.7	6.7	6.7	33.3	6.7	6.7	13.4	53.3
PMMA-SF$_6$ (×1)	7.2	6.7	9.7	11.9	3.2	-	38.8	4.1	4.3	8.4	52.8
PMMA-SF$_6$ (×5)	12.5	6.6	8.8	11.5	2.7	-	42.3	4.7	3.5	8.2	49.5
PMMA-SF$_6$ (×1) 15 days	15.7	9.7	9.4	9.7	2.5	-	47.0	6.1	4.1	10.2	42.8

The C1s peak shows the three theoretical components (Figure 4A). However, as expected from the deficiency in the oxygen content discussed above, we also observed a higher amount of aliphatic carbon (C–C component).
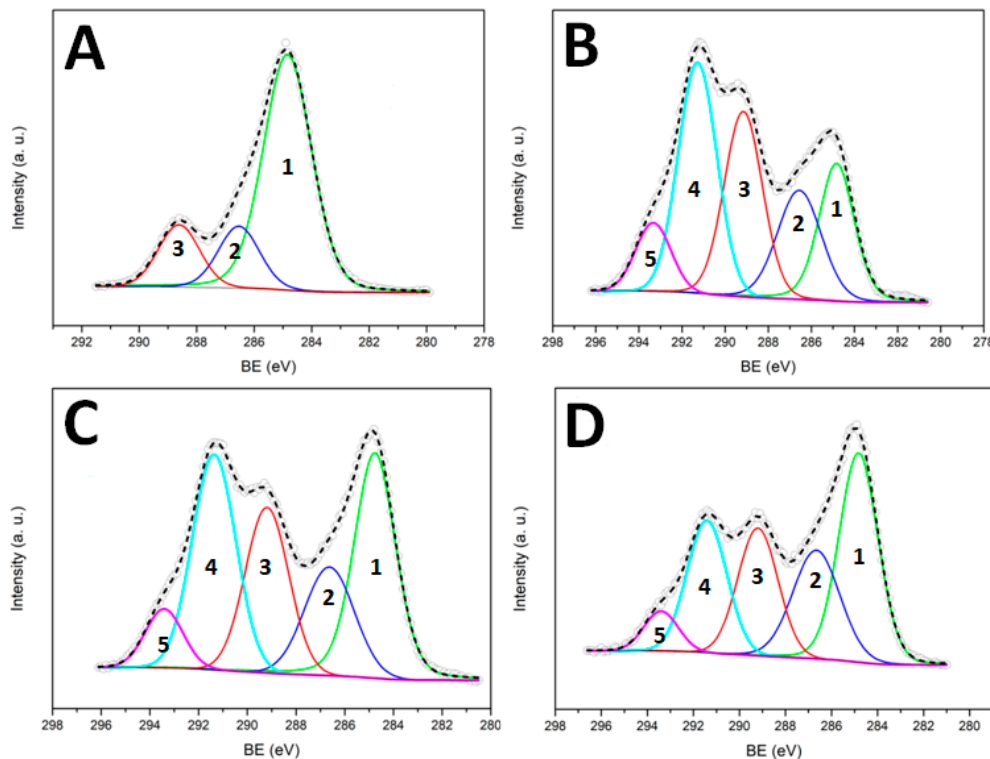
Figure 4. C1s peak deconvolution for untreated PMMA (**A**), PMMA treated one time (**B**), PMMA treated five times (**C**) and PMMA treated one time and stored in air for 15 days (**D**). The five components refer to: *C–C* (1), *C–O/C–CF* (2), *C=O/CF* (3), *CF*$_2$ (4), *CF*$_3$ (5).

The surface composition of the sample subjected to plasma treatment in the selected conditions (peak power = 70 W, SF$_6$ pressure = 30 Pa, DC = 50%) differs from that of a theoretical fully fluorinated PMMA. In particular, the oxygen percentage is only 60% of the theoretical one. We suggest this is due to lateral chains loss, owing to the plasma bombardment. Another important difference between the theoretical and the measured values in the absence of an O–CF$_3$ component in the high-resolution C1s peak. According to the literature [25], this component should occur at higher Binding Energy (BE) with respect to the C–CF$_3$, but it did not appear in our spectra. Surface fluorination in an SF$_6$ plasma is not a selective process: in our case, we should expect insertion of fluorine in the polymer backbone as well as in the methoxy group of the methyl ester. The absence of O–CF$_3$ groups can be explained by their instability when subjected to the plasma species bombardment. Loss of·O–CF$_3$ and/or·CF$_3$ radicals can be hypothesized, with the formation of acyl and carboxyl acid radicals, respectively (see Figure 5). These radicals can undergo loss of CO and CO$_2$, respectively, in agreement with the low oxygen percentage detected onto the plasma-treated sample.

Other important information can be obtained by observing the C1s and O1s deconvolution results in Table 1. First of all, while the total oxygen percentage is lower than the theoretical one, the oxidized components of the C1s peak appear to be equal (*C–O*) or even greater (*C=O*) than those predicted. This anomaly is a consequence of the surface fluorination, because the carbon-based components *C*–CF$_3$ and *C*-F have a BE close to that of C–O and C=O, respectively [25,26]. Secondly, from the C1s deconvolution, it appears that the CF$_2$ component is greater than the theoretical one, while the CF$_3$ is smaller. Two reasons can contribute to this result: an incomplete fluorination of the CH$_3$ group of the methacrylate (formation of –CF$_2$H groups) and the cross-linking of two neighbouring chains, involving the same group. In the latter case, the formation of –C–CF$_2$–C- and –C–CF$_2$–CF$_2$–C– groups can be hypothesized.
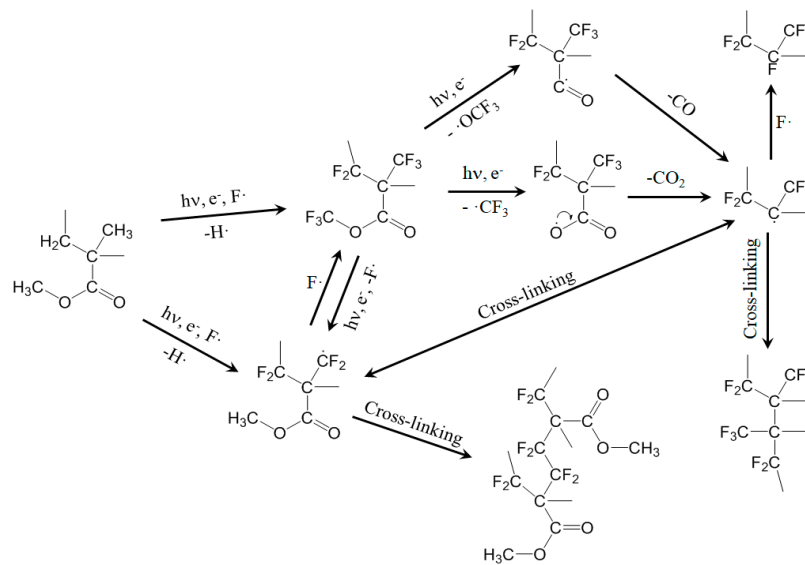

Figure 5. Proposed mechanism for the plasma fluorination of PMMA.

Figure 5 proposes some possible reactions involved in the plasma fluorination of PMMA, explaining the loss of lateral chains, the cross-linking and the formation of CF$_2$ and CF groups.

3.1.4. Ageing Effects

The optimization of the surface modification protocol must consider possible ageing effects (variations of the surface chemical composition with the ageing time). In our case, we noticed that the surface hydro-repellence of the treated samples decreased with the ageing time (Table 2). This phenomenon is not unusual since it was already observed in the past for SF_6 plasma treatment of other materials and, more generally, for several kinds of plasma-treated surfaces [14]. It is generally accepted that the ageing phenomenon is due to surface adaptation (rearrangement motions that move some of the polymer chains from the surface into the bulk, in response to interfacial energy differences between the treated surface and its environment). Here, because of these motions, superficial fluorinated chains of the PMMA migrate into the bulk, exposing on the surface the polymer chains which do not contain fluorine. This was confirmed by XPS analyses. Table 1 and Figure 4D show the XPS results for a plasma-treated PMMA IOL (peak power = 70 W, SF_6 pressure = 30 Pa, DC = 50%) stored for 15 days in air. Compared with the freshly prepared sample, this one displayed a lower percentage of fluorine and a higher percentage of oxygen, as a consequence of the motion of fluorinated chains inside the polymer bulk (the penetration depth of the XPS analysis is few nanometers). Moreover, the C–C component became predominant in the C1s peak due to migration of non-fluorinated chains towards the PMMA/air interface.

The surface rearrangement is promoted by the contact with humid air, and it indicates (indirectly) the low cross-linking degree of a PMMA sample subjected to one SF_6 plasma treatment. Table 2 shows also the advancing and receding contact angles measured onto PMMA IOLs treated in the selected conditions (peak power = 70 W, SF_6 pressure = 30 Pa, DC = 50%) and then stored in two different environments.

Table 2. Contact angle ageing of the plasma-treated samples.

Sample	θ_{adv}	θ_{rec}
Untreated PMMA	93°	22°
Plasma treated PMMA (70 W - 30 Pa)	114°	54°
Plasma treated PMMA after 3 days in air	96°	20°
Plasma treated PMMA after 3 days in vacuum chamber	113°	55°
Plasma treated PMMA after 30 days in air	86°	18°
Plasma treated PMMA (×5) after 30 days in air	105°	38°

As expected, while the sample stored in air displayed a decrease of contact angles, the one stored under vacuum conditions did not suffer from ageing, and contact angles measured after three days were equal to those measured immediately after the plasma treatment.

In order to overcome (or to limit) the ageing effects, we started from the hypothesis that chains motion plays a crucial role in the contact angles decrease. Following this hypothesis, we tested the repetition of SF_6 plasma treatments on the same sample. The PMMA lens was plasma treated in the selected conditions (peak power = 70 W, SF_6 pressure = 30 Pa, DC = 50%) and then stored in air for 24 h to allow the migration of the fluorine-containing chains inside the polymer bulk. Consequently, polymer segments which do not contain fluorine atoms are exposed on the PMMA/air interface. The ageing of the treated lens during this short ageing time was assessed by contact angle measurements. The lens was then treated again in the same conditions. The "fresh" surface undergoes fluorination, followed by new ageing with fluorine migration inside the polymer bulk, and so on. The treatment/ageing alternation was repeated five times. In this way, we expected to extend the fluorination to a much deeper surface layer, as already observed in the past for poly(ethylene terephthalate) [15]. Surprisingly, XPS analysis performed on the PMMA sample after the fifth plasma treatment shows a surface percentage of fluorine comparable (or even less) to that measured on a single-treated sample and a higher C–C component of the C1s peak. This can be interpreted in terms

of a partial loss of CF$_3$ groups due to the repetition of the treatment. The loss of these groups, together with that of lateral chains, contributes to increasing the degree of cross-linking, helping to overcome the ageing effects. As with the single-treated lens, the multi-treated lens was stored in air for 30 days. Table 2 shows the contact angles measured for both of these lenses. It is worth noticing that the multi-treated lens maintains good hydrophobic properties 30 days after the plasma treatments. This agrees with the formation of a highly cross-linked and totally fluorinated layer, which displays a Teflon-like composition due to the essential loss of oxygenated functionalities (see the proposed mechanism in Figure 5).

3.1.5. Topography and Transparency

For IOLs, transparency is obviously a required characteristic. However, it is well known that, depending on the process parameters, etching effects can occur during plasma treatment of polymers with fluorinated gases such as SF$_6$. Etching can increase the surface roughness of the polymeric substrate which, in turn, can decrease its transparency. In order to investigate if our treatment has such detrimental effects, we evaluated both the topography and the transparency of the IOLs before and after the plasma treatment.

Figure 6 shows the AFM images of the untreated (Figure 6A,B) and the plasma treated (Figure 6C,D) PMMA (peak power = 70 W, SF$_6$ pressure = 30 Pa, DC = 50%).
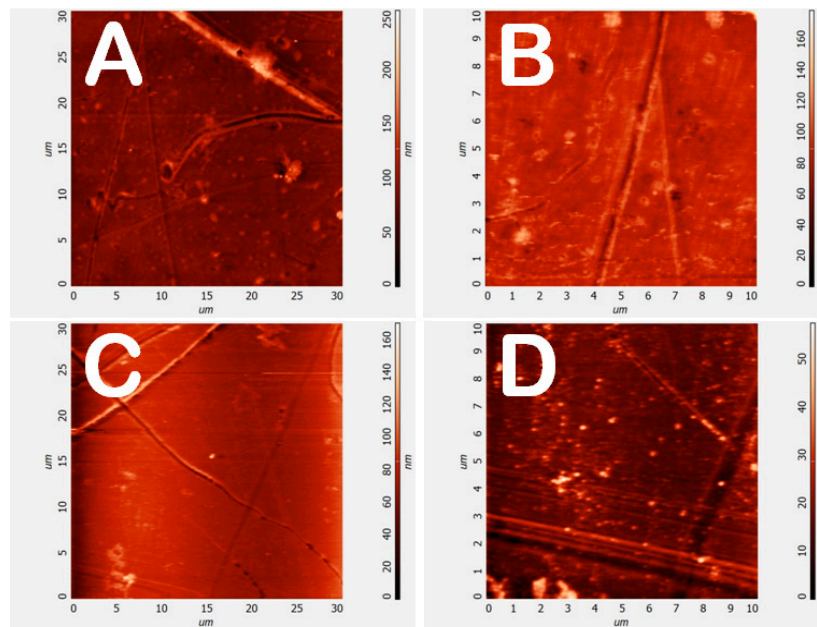

Figure 6. Atomic Force Microscopy (AFM) images of untreated (**A** and **B**) and plasma treated (**C** and **D**) PMMA lenses (peak power = 70 W, SF$_6$ pressure = 30 Pa, DC = 50%).

No appreciable differences were detected, and the root means square values of the heights measured for untreated and plasma-treated surfaces are comparable (Table 3). This is a further indication of the mild character of this plasma-based approach, in which grafting of fluorine atoms prevail over-etching effects.

Table 3. Root mean square (r.m.s.) of the heights for untreated and plasma treated samples (peak power = 70 W, SF_6 pressure = 30 Pa, DC = 50%).

Sample	r.m.s. 10 × 10 μm²	r.m.s. 30 × 30 μm²
Untreated	8.8 nm	16.4 nm
Plasma treated	5.4 nm	13.7 nm

The transparency of the plasma-treated lenses was confirmed by UV/VIS spectra (Figure 7), which displayed a negligible decrease in the transmittance in the range 430–800 nm. However, a significant decrease (about 25%) in the transmittance in the UV-violet range (300–430 nm) was observed. It is noteworthy that the maximum decrease of transmittance occurs below 400nm so in violet-blue and UV region while practically the same transmittance is observed in the visible or infrared region underlining that the plasma fluorination can produce UV filtering species at the PMMA surface. This aspect is of great importance in optical ocular devices since the UV or violet-blue radiation is responsible for retina ageing or retina pathologies [27,28]. This effect was previously observed for fluorinated methacrylate polymers [29] and could open the interesting application of this plasma treatment for the creation of UV filter in ophthalmic optical devices (glasses, contact lenses and IOLs).
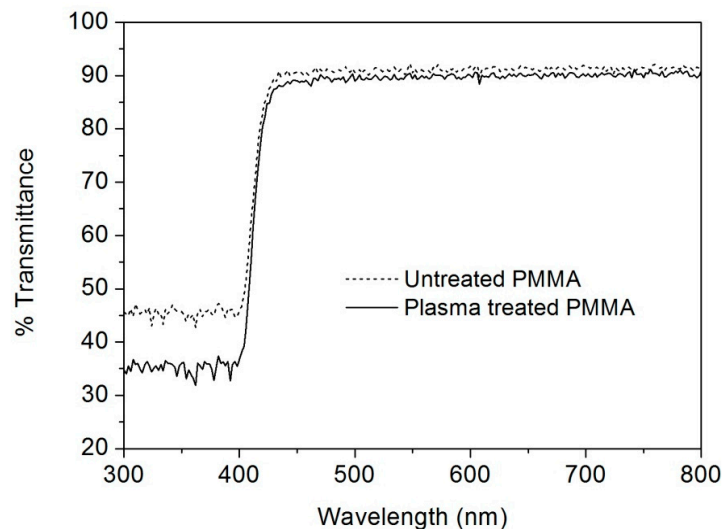

Figure 7. UV/VIS transmittance spectra of untreated (dash line) and plasma-treated (full line) PMMA lenses (peak power = 70 W, SF_6 pressure = 30 Pa, DC = 50%).

3.2. Immersion Studies Results

A range of PMMA samples was subjected to immersion studies which involved the sample being immersed in a SAH solution for 8 weeks to test how well the treated samples hindered inorganic salts deposition compared to untreated (control) samples.

The samples used for the immersion study were plasma treated once a day, for 5 days (PMMA-$SF_6 \times 5$ in Table 1). In these five days, samples A were stored in air at room temperature, while samples B were stored in an oven at 50 °C (with a beaker of water, to increase the humidity and force the migration of the fluorine-containing chains inside the polymer bulk).

Table 4 shows the contact angles measured 4 days after the final plasma treatment. Data of untreated PMMA are also shown for comparison prior to immersion.

Table 4. Contact angle of the samples used for immersion studies.

Sample	Angle Advancing (°)	Angle Receding (°)
Untreated PMMA	93	22
A1	124	60
A2	104	33
B1	120	55
B2	118	57

The modified samples showed an increase in the contact angle surface tension compared to the unmodified sample, suggesting that the surface has become more hydrophobic and in theory, this should, therefore, prevent deposits from adhering to the surface of these samples.

The aim of this study was to look at aspects of the opacification process resulting from the immersion of lenses in Simulated Aqueous Humour (SAH). XPS analysis was used to investigate the inorganic nature of material deposited on the surface both untreated and fluorinated samples. After immersion, the untreated PMMA sample shows a greater percentage of deposit elements than all the plasma-treated fluorinated samples. For the treated samples the fluorine percentages are lower than for sample that has not been subjected to immersion studies (Table 5) because the presence of the deposited layer means that photoelectron emission from the modified PMMA that is detected is reduced. The greater percentage of carbon in the fluorinated samples also suggests a thinner layer of inorganic deposit on the surface than for the untreated sample (the sampling depth of XPS is typically less than 5 nm). The atomic percentages, therefore, suggest that the deposition has penetrated deep into the untreated sample. The large reduction in percentage fluorine seen (from 50% to 2.46%) suggests that emissions in the XPS are predominantly arising from the deposited layer and very little of the original surface is contributing to the signal detected. The oxygen observed in the XPS is expected to be mainly due to the phosphate deposit, 5% phosphorous would be expected to contribute about 20% oxygen. The carbon percentage suggests organic deposits from the SAH are also present on the surface after immersion. The deposits are thought to mainly consist of NaCl and Calcium phosphates ($Ca_3(PO_4)_2$). As the sodium percentages are consistently higher than that of chlorine, other sodium-containing deposits are likely to be present. In previous works regarding gas fluorinated PMMA samples immersed in SAH (8 weeks), the EDS analysis indicated the presence of sodium chloride crystallites but a negligible calcium deposition [10,30]. This previous result could be attributed to the concentration of NaCl in the SAH being > ×50 higher than that calcium and phosphate. The SF_6 plasma treatment used for samples tested here seems to be much less effective at preventing calcium phosphate deposition. This is surprising given that the XPS data indicates that the PMMA surface is nearly completely fluorinated. One reason for the difference is that gas fluorination tends to produce a thicker fluorinated layer than plasma treatment and this may be the reason for the prevention of inorganic deposits in gas treated samples.

Table 5. XPS data for untreated and plasma-treated PMMA samples after immersion in Simulated Aqueous Humour (SAH).

Sample	% C	% O	% F	% Ca	% P	% Na	% Cl
Un-treated PMMA (1)	24.25	43.7	-	12.49	10.96	3.65	3.91
Un-treated PMMA (2)	36.33	37.24	-	10.06	7.86	5.12	3.39
Un-treated PMMA (3)	21.13	43.41	-	9.38	11.04	9.1	5.95
Fluorinated PMMA A1	27.80	33.45	2.46	7.14	6.76	7.14	6.76
Fluorinated PMMA A2	30.48	37.88	2.64	7.09	6.76	7.09	6.76
Fluorinated PMMA B1	28.92	33.56	3.89	6.61	6.74	6.61	6.74
Fluorinated PMMA B2	18.72	29.08	1.97	6.23	5.94	6.23	5.94

4. Conclusions

Surface fluorination of medical-grade PMMA was successfully attained by SF₆ plasma treatment. When optimal plasma conditions were employed, treated samples showed an increased hydrophobicity compared to the unmodified sample. Moreover, the mild character of the plasma treatment allowed the grafting of fluorine atoms with no etching effects (no morphological damaging of the PMMA surface). The repeated fluorination seems to be an important strategy for stabilizing the hydrophobic surface properties. The latter seems to be related to the formation of an extended perfluorinated layer on the surface, a layer which seems to exhibit also peculiar optical properties. Indeed, the transparency of the plasma-treated lenses was maintained in the visible range, while an important decrease (about 25%) of the transmittance in the UV-violet range (300-430 nm) was detected. This last result could open the interesting application of this treatment for the creation of UV filter in ophthalmic optical devices. Finally, when immersed in Simulated Aqueous Humour (SAH), the modified samples showed averagely less inorganic deposit on the surface than the unmodified sample. Particularly in samples B1 and B2 (stored in an oven at 50°C post-treatment).

Conflicts of Interest: The authors declare no conflict of interest.

References

1.　Kohnen, T. The Variety of Foldable Intraocular Lens Materials. *J. Cataract Refract. Surg.* **1996**, *22*, 1255–1258.
2.　Werner, L. Calcification of Hydrophilic Acrylic Intraocular Lenses. *Am. J. Ophthalmol.* **2008**, *146*, 341–343.
3.　Werner, L. Causes of Intraocular Lens Opacification or Discoloration. *J. Cataract Refract. Surg.* **2007**, *33*, 713–726.
4.　Dalas, E.; Kallitsis, J.K.; Koutsoukos, P.G. Crystallization of Hydroxyapatite on Polymers. *Langmuir* **1991**, *7*, 1822–1826.
5.　Bucher, P.J.; Büchi, E.R.; Daicker, B.C. Dystrophic calcification of an implanted hydroxyethylmethacrylate intraocular lens. *Arch. Ophthalmol.* **1995**, *113*, 1431–1435.
6.　Olson, R.J.; Caldwell, K.D.; Crandall, A.S.; Jensen, M.K.; Huang, S.-C. Intraoperative Crystallization on the Intraocular Lens Surface. *Am. J. Ophthalmol.* **1998**, *126*, 177–184.
7.　Zainuddin; Chirila, T.V.; Hill, D.J.T.; Whittaker, A.K. Study of the Calcification of PHEMA Hydrogels Using a Two Compartment Permeation Cell. *J. Mol. Struct.* **2005**, *739*, 199–206.
8.　Moghbelli, E.; Banyay, R.; Sue, H.-J. Effect of Moisture Exposure on Scratch Resistance of PMMA. *Tribol. Int.* **2014**, *69*, 46–51.
9.　Ghatora, B.K.; Foot, P.J.S.; Barton, S.J.; Thatti, R.S.; Papagni, A.; Vaghi, L. Surface Perfluoroalkyl Chains Segregation: A Tool for Reducing Calcium Deposits in Medical Grade Poly(Methyl Methacrylate). *J. Biomater. Nanobiotechnol.* **2017**, *8*, 176–187.
10.　Ghatora, B.K.; Barton, S.J.; Foot, P.J.S.; Tate, P.M. The Effect of Direct Gas Fluorination on Medical Grade Poly(methyl Methacrylate). *Open J. Org. Polym. Mater.* **2014**, *4*, 74–83.
11.　Zanini, S.; Ziano, R.; Riccardi, C. Stable Poly(Acrylic Acid) Films from Acrylic Acid/Argon Plasmas: Influence of the Mixture Composition and the Reactor Geometry on the Thin Films Chemical Structures. *Plasma Chem. Plasma Process.* **2009**, *29*, 535–547.
12.　Zanini, S.; Zoia, L.; Dell'Orto, E.C.; Natalello, A.; Villa, A.M.; Pergola, R.D.; Riccardi, C. Plasma Polymerized 2-Ethyl-2-Oxazoline: Chemical Characterization and Study of the Reactivity towards Different Chemical Groups. *Mater. Des.* **2016**, *108*, 791–800.

13. Taraballi, F.; Zanini, S.; Lupo, C.; Panseri, S.; Cunha, C.; Riccardi, C.; Marcacci, M.; Campione, M.; Cipolla, L. Amino and Carboxyl Plasma Functionalization of Collagen Films for Tissue Engineering Applications. *J. Colloid Interface Sci.* **2013**, *394*, 590–597.

14. Siow, K.S.; Britcher, L.; Kumar, S.; Griesser, H.J. Plasma Methods for the Generation of Chemically Reactive Surfaces for Biomolecule Immobilization and Cell Colonization - A Review. *Plasma Process. Polym.* **2006**, *3*, 392–418.

15. Selli, E.; Mazzone, G.; Oliva, C.; Martini, F.; Riccardi, C.; Barni, R.; Marcandalli, B.; Massafra, M.R. Characterisation of Poly(ethylene Terephthalate) and Cotton Fibres after Cold SF6 Plasma Treatment. *J. Mater. Chem.* **2001**, *11*, 1985–1991.

16. Barni, R.; Riccardi, C.; Selli, E.; Massafra, M.R.; Marcandalli, B.; Orsini, F.; Poletti, G.; Meda, L. Wettability and Dyeability Modulation of Poly(ethylene Terephthalate) Fibers through Cold SF_6 Plasma Treatment. *Plasma Process. Polym.* **2005**, *2*, 64–72.

17. Barni, R.; Zanini, S.; Beretta, D.; Riccardi, C. Experimental Study of Hydrophobic/Hydrophilic Transition in SF_6 plasma Interaction with Polymer Surfaces. *Eur. Phys. J. Appl. Phys.* **2007**, *38*, 263–268.

18. Selli, E.; Riccardi, C.; Massafra, M.R.; Marcandalli, B. Surface Modifications of Silk by Cold SF_6 Plasma Treatment. *Macromol. Chem. Phys.* **2001**, *202*, 1672–1678.

19. Chirila, T.V.; Morrison, D.A.; Gridneva, Z.; Meyrick, D.; Hicks, C.R.; Webb, J.M. Effect of Multipurpose Solutions for Contact Lens Care on the in Vitro Drug-Induced Spoliation of poly(2-Hydroxyethyl Methacrylate) in Simulated Aqueous Humour. *Cont. Lens Anterior Eye* **2005**, *28*, 21–28.

20. Zanini, S.; Grimoldi, E.; Riccardi, C. Development of Controlled Releasing Surfaces by Plasma Deposited Multilayers. *Mater. Chem. Phys.* **2013**, *138*, 850–855.

21. Briggs, D.; Seah, M. In *Practical Surface Analysis*. Wiley, Chichester, UK, 1990.

22. Shirley, D.A. High-Resolution X-Ray Photoemission Spectrum of the Valence Bands of Gold. *Phys. Rev. B* **1972**, *5*, 4709–4714.

23. Moulder, J.F.; Stickle, W.F.; Sobol, P.E.; Bomben, K.D. *Handbook of X-ray Photoelectron Spectroscopy, Physical Electronics*; Physical Electronics Division: Eden Prairie, MN, USA, 1992.

24. Ryan, M.E.; Fonseca, J.L.C.; Tasker, S.; Badyal, J.P.S. Plasma Polymerization of Sputtered Poly(tetrafluoroethylene). *J. Phys. Chem.* **1995**, *99*, 7060–7064.

25. Ferraria, A.M.; Lopes da Silva, J.D.; Botelho do Rego, A.M. XPS Studies of Directly Fluorinated HDPE: Problems and Solutions. *Polymer* **2003**, *44*, 7241–7249.

26. Haïdopoulos, M.; Turgeon, S.; Laroche, G.; Mantovani, D. Chemical and Morphological Characterization of Ultra-Thin Fluorocarbon Plasma-Polymer Deposition on 316 Stainless Steel Substrates: A First Step Toward the Improvement of the Long-Term Safety of Coated-Stents. *Plasma Process. Polym.* **2005**, *2*, 424–440.

27. Youssef, P.N.; Sheibani, N.; Albert, D.M. Retinal Light Toxicity. *Eye* **2010**, *25*, 1–14.

28. Logan, P.; Bernabeu, M.; Ferreira, A.; Burnier, M.N. Evidence for the Role of Blue Light in the Development of Uveal Melanoma. *J. Ophthalmol.* **2015**, *2015*, 1–7.

29. Gaynor, J.; Schueneman, G.; Schuman, P.; Harmon, J.P. Effects of Fluorinated Substituents on the Refractive Index and Optical Radiation Resistance of Methacrylates. *J. Appl. Polym. Sci.* **1993**, *50*, 1645–1653.

30. Padilha, G. da S.; Giacon, V.M.; Bartoli, J.R. Effect of Plasma Fluorination Variables on the Deposition and Growth of Partially Fluorinated Polymer over PMMA Films. *Polim. Cienc. Tecnol.* **2013**, *23*, 585–589.